Vol. 39(1), pp. 21-31, June 2020
ISSN 1821-536X (print)
ISSN 2619-8789 (electronic)

Tanzania Journal of Engineering and Technology
Copyright © 2020 College of Engineering and Technology, University of Dar es Salaam

Full Length Research Paper

Comminution Characteristics of Lithium Bearing Mica Ores From Different Devices

A. Wikedzi [1,2*], T. Leißner [1], T. Fraszczak[1], U. A. Peuker[1] and T. Mütze[1]

[1] TU Bergakademie Freiberg, Institute of Mechanical Process Engineering and Mineral Processing, Agricolastraße 1, 09599 Freiberg/Germany
[2] Chemical and Mining Engineering, University of Dar es Salaam, Tanzania

*Corresponding Author: alpho20012001@gmail.com

ABSTRACT

This paper highlights on the comminution and to the lesser extent liberation properties of two greisen-type lithium bearing-mica ores (L1, L2) subjected to different breakage devices; cone crusher (CC), roller crusher (RC), rotor beater mill (RBM) and a screen mill (SM). The particle size distributions (PSD) of the products from each device were evaluated to search for an appropriate PSD model using Gates-Gaudin-Schuhmann (GGS) and Rosin-Rammler (RR) functions. To determine an appropriate function, coefficients of determination (R^2) were used as a criterion. Due to budget constraint, only products from rotor beater mill (RBM) were examined for mineral liberation by an automated scanning electron microscope (SEM) technique. It was found that RBM, RC and SM products were better described by the RR model than the GGS model with higher R^2 values of 0.97 to 1.0. However, cone crusher products for L1 were better described by GSS model, while that for L2 were better described by RR model. In terms of the spread of size distribution as indicated by RR model parameters, RC products were more uniformly distributed compared to those from other devices, for both ores. Also the RBM products were more scattered than those from other devices. The results indicate that the composition of individual ores affected the comminution products PSDs as different PSD model parameters were obtained for samples comminuted by same devices. The modal mineralogy indicated that both ores are rich in quartz, topaz, zinnwaldite and muscovite. Furthermore, the result indicates that, for both ores, the zinnwaldite phase is more enriched in the fraction < 250 µm. Moreover, better liberation of zinnwaldite is observed for L1 compared to L2. This could be explained by differences of the two ores in three aspects; the nature of mineral association, reduction ratio of the fractions analysed and the spread of the size distribution.

Keywords: *Comminution, mineral liberation, Rosin-Rammler distribution, particle size distribution, Gates-Gaudin-Schuhmann distribution.*

INTRODUCTION

In mineral processing, particle size is a critical parameter specifically for the liberation and separation of minerals. Assessing the particle size distribution of the ore, which is processed in different stages such as crushing and grinding, is critical for the productivity control of the total mining operation (Kursun, 2009). Amongst other uses, the knowledge of particle size is applied in the development of sampling protocols which in turn feeds into quality control. However, particle size distribution (PSD) parameters are employed in modelling and simulation of comminution unit operations. Furthermore, the models described for plant equipment, such as cyclones or flotation cells, require knowledge of particle size as an input (Taşdemir and Taşdemir, 2009).

The characteristics of size distributions from comminution processes may depend on several factors; the extent of comminution mechanisms applied by devices, comminution conditions, initial ore characteristics, as well as whether a size classification system is applied or not. Furthermore, comminution conditions that favor one breakage mode over the other may be critical in determining the size distribution of products (Taşdemir and Taşdemir, 2009). In comminution, different fracture mechanisms exist such as impact or compression, abrasion or attrition and cleavage. These mechanisms normally occur in combination (Rao, 2011) and their relative predominance varies as a function of machine type, operating conditions and the material being comminuted (Christelle *et al.*, 1997).

In crushing operations the size reduction is more by compression and impact and less of attrition or abrasion, while in grinding the attrition forces are much greater in addition to the impact (Gupta and Yan, 2006) forces. The combination of the above types of fragmentation mechanisms yield different product characteristic of the ground material, since each type is active to a different extent with different machines and materials (Gupta and Yan, 2006; Rao, 2011). In principle, jaw and cone crushers are the most common types of primary compression crushers. These are essentially considered as single-pass devices as can offer limited retention time for the broken materials. On the other hand, hammer crushers and ball mills are considered as retention type devices as they offer repeated particle breakage (Kaya *et al*., 2002).

Most mineral processing operations rely on measurements of size distributions, as a key factor in improving comminution efficiency. The size distribution of ground materials is typically skewed and the normal distribution is uncommon and occurs only for narrow size ranges (Allen, 2003). Hence, several equations have been proposed to describe size distributions of comminution products (Narayanan and Whiten, 1983). The most important functions have been reviewed by Allen (2003) and King (2001) and due to their simplicity and accuracy, Rosin–Rammler (RR) and Gates–Gaudin–Schuhmann (GGS) are recommended as the two most applicable models for description of comminution products for different materials. Furthermore, the two models are particularly suited for representing size distributions of products from crushing and grinding operations (Macías-García *et al*., 2004).

It is well known that the efficiency of any comminution process need to be measured not only based on size reduction, but also on the degree of mineral liberation achieved as the two are inextricably linked. If the size to which the rock is reduced is insufficient, then a relatively large proportion of the valuable constituents will not be extracted, leading

to loss of potential revenue. If the size chosen is too small, this will result to an oversized and over costly plant with unnecessarily high energy costs (Napier-Munn *et al*., 1996).

Limited studies have been reported on breakage and liberation characterization of Lithium-bearing mica ores of the greisen-type deposits. Therefore, this work summarizes the comminution and to a less extent the liberation properties of two greisen-type lithium bearing-mica ores (i.e. L1 and L2) subjected to different comminution devices; cone crusher (CC), roller crusher (RC), rotor beater mill (RBM) and a screen mill (SM). The particle size distributions (PSD) of the products from each device were evaluated using Gates-Gaudin-Schuhmann (GGS) and Rosin-Rammler (RR) models. The choice of the two models was motivated by their simplicity as well as accuracy as reported from literature. Also, the use of these models is aimed at demonstrating another scientific example where they can be applicable. The coefficients of determination (R^2) were used as a criterion in recommending a suitable model that could well describe the experimental data of the investigated ore materials. Due to budget constraint, only the products from rotor beater mill (RBM) were examined for mineral liberation characteristics of the two ores by an automated scanning electron microscope (SEM) technique. Furthermore, it is anticipated that the suitable model (RR or GGS) could be applied in modelling and simulation studies of typical materials.

MATERIALS AND METHODS

Materials

Two greisen-type lithium bearing-mica ores (i.e. L1 and L2) originating from the same deposit (i.e. Zinnwald/Cinovec) at the German-Czech border were used in this investigation. The mineralogical composition of the two ores based on mineral liberation analysis is presented in Table 1. Quartz is the main gangue in both samples and on the other side, the differences in the content of Lithium bearing Zinnwaldite phase for the two samples is significant. The ‘’other’’ category consists of minor phases with sulphates, silicates, sulphides and fluorides. More detailed information on the ore can be seen from the existing literature (Leißner *et al*., 2012; Sandmann and Gutzmer, 2013).

Table1: Modal mineralogy of the two samples

Mineral	L1 (wt %)	L2 (wt %)
Quartz	71.37	72.99
Topaz	7.48	6.37
Zinnwaldite	16.14	3.2
Muscovite	2.99	16
Limonite / Columbite	0.16	0.02
Other	1.87	1.43
Total	**100**	**100**

Comminution tests

The samples were subjected to different breakage equipment such as cone crusher (CC), roller crusher (RC), rotor beater mill (RBM) and a screen mill (SM). Figure 1 presents all comminution tests involved. The roll crusher (RC) gap was set at 1 mm and both, the rotor beater mill (RBM) and screen mill (SM) were operated with a

1.4 mm screens. Other parameters for the screen mill were: Diameter, D (0.39 m), Length, L (0.175 m), speed (55 rpm), media filling degree, φ_{GM} (0.5), void filling (100 %) and powder filling degree, φ_{MG}(0.2).

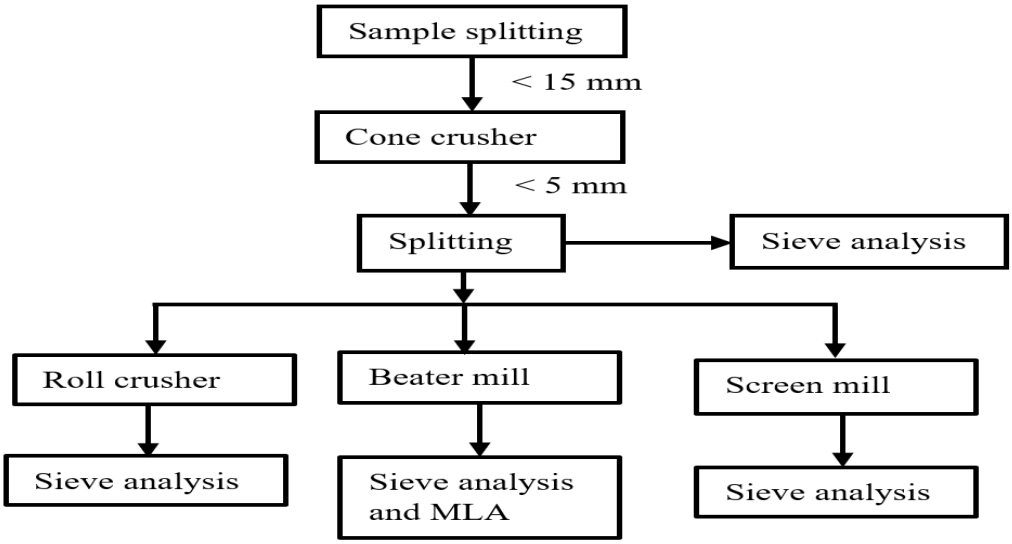

Figure 1: Block diagram for the comminution tests conducted.

Mineral Liberation Studies

The liberation characteristics of the two Lithium bearing-mica ores was determined by an automated mineral liberation analysis (MLA) technique using FEI MLA 600F system (Sandmann and Gutzmer, 2013). As a consequence of costs, only products from rotor beater mill (RBM) were examined in this case. Therefore, rotor beater mill products were sieved into five fractions, +0.5 mm, -0.5 +0.315 mm, -.315 +0.2 mm, -0.2 +0.1 mm and -0.1 mm, which were given to an automated mineralogical characterization technique.

The five fractions were necessary and chosen based on the standard particle size range suitable for measurements by an Automated Scanning Electron Microscope (SEM). Before feeding to the system, the samples were prepared as polished grain mounts (Leißner *et al*., 2016b; Sandmann and Gutzmer, 2013). The mounts were carbon-coated prior to measurements in order to obtain an electrically conducting surface. The analysis of mineral liberation data was performed using MLA Dataview (Fandrich *et al*., 2007).

Gates-Gaudin-Schuman (GGS) Distribution

The GGS distribution is given in equation (1) as described by Gupta and Yan (2006).

$$y = 100\left[\left(\frac{x}{k}\right)^{a}\right] \quad \text{.....(1)}$$

Where x is screen aperture size, y is the cumulative mass % passing size x, k is the size parameter and a is the distribution parameter (spread of distribution). The two parameters characterize the size of the sample. Theoretically, lower values of a indicate more fines, more large particles and fewer particles in the middle range (Lu *et al*., 2003). The higher the value of a, the narrower the distribution. The size parameter, is the measure of the top size (Gupta and Yan, 2006).

Equation (1) can be transformed to linear form by applying logarithms on both sides, giving:

$$\log\left(\frac{y}{100}\right) = a \log x + \text{constant} \quad \ldots\ldots\ldots (2)$$

This is an equation of a straight line if x and y are plotted in a log-log scale. The slope of the straight line will be the distribution parameter, a, and the intercept of the straight line, when $y = 100$, will be the size parameter, k.

Rosin-Rammler (RR) Distribution

The Rosin-Rammler (or Weibull) distribution is expressed in equation (3) (Gupta and Yan, 2006; King, 2001):

$$R = 100 \exp\left[-\left(\frac{x}{x'}\right)^b\right] \quad \ldots\ldots\ldots\ldots\ldots (3)$$

Where R is the cumulative mass % retained on size x, x' is the size parameter and b is the distribution parameter. Small values of b indicate a scattered distribution, and large values imply uniform distribution (Manohar and Sridhar, 2001). Rearranging and taking logarithm of both sides of equation (3) gives equation (4).

$$\log\left(\frac{100}{R}\right) = \left(\frac{x}{x'}\right)^b \log e \quad \ldots\ldots\ldots\ldots\ldots (4)$$

Taking logarithms, a second time to remove the exponent gives:

$$\log\log\left(\frac{100}{R}\right) = b \log x + \text{constant} \quad \ldots. (5)$$

A plot of log log (100/R) versus log x should give a straight line. The parameters of the Rosin-Rammler distribution, b and x' are obtained from the slope of the straight line and the intercept at the horizontal line at $R = 36.8$, respectively.

The model parameters for both RR and GSS functions (equations (2) and (5)) were calculated by a non-linear regression technique using SOLVER function in EXCEL. The method searches for the best combination of the fitting parameters of a model by minimization of residual error between experimental size distributions and the predicted values (Katubilwa and Moys, 2009; Sand and Subasinghe, 2004).

RESULTS AND DISCUSSION

The results of the two aspects investigated (i.e. comminution and liberation characteristics) for the two greisen-type lithium bearing-mica ores are presented in following sections.

Comminution Characterization

Figure 2(a) presents the size distributions of the two samples (L1 and L2) after comminution with cone crusher. Minor differences can be observed in terms of feed size distributions for the two samples. In terms of products, sample L1 gave finer product than sample L2. The products from the cone crusher were used as feed to different comminution devices of which the products size distributions are shown in Figure 2(b). In this case, comminution products from screen mill (SM) were the finest (i.e. sample L2 followed by sample L1). These were closely followed by comminution products from the rotor beater mill (RBM) (i.e. L1 followed by L2). The comminution products from the roller crusher (RC) were the coarsest (i.e. L2 followed by L1).

The differences in products fineness for the different comminution devices applied can be explained as follows. The single-pass devices such as Jaw and cone crushers can offer limited retention time for the breakage of particles, contrary to the retention type devices such as rotor beater mill, roll crusher, hammer crusher and ball mill which can offer significant retention times, providing repeated breakage events (Yue and Klein, 2005). Hence, the former will give coarser products and the later finer products as experienced in this study.

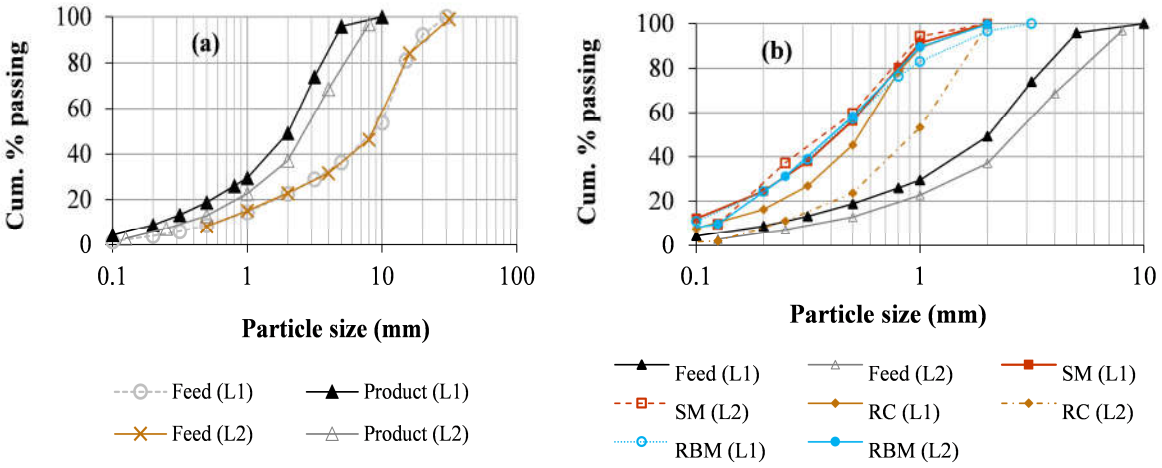

Figure 2: (a) Products size distributions after cone crusher comminution. (b) PSD based on different comminution devices (RC=Roll crusher, RBM=Rotor beater mill, and SM=Screen mill).

The size distributions of products from different comminution devices (Figure 2(b) were fitted into GSS and RR models, Equations (2) and (5) and the results of model parameters as well as coefficients of determination are presented in Table 2 and Table 3 for GGS and RR models, respectively. Based on values of coefficients of determination (R^2), it is seen that the rotor beater mill (RBM), roller crusher (RC) and screen mill (SM) products are better described by RR model than the GGS model with higher R^2 values (0.97-1.0). However, it is only the cone crusher product for L1 that is better described by the GSS model. Furthermore, for all devices, the coefficients of determination (R^2) for L2 products described by GGS model are slightly smaller than those obtained when the same material is described by RR model. This indicates that, RR function fits better for description of wider size distributions (Yue and Klein, 2005) as the case for L2 products.

Table 2: GGS parameters for the two samples as comminuted by different devices

	L1			L2		
Device	*a*	*k*	R^2	*a*	*k*	R^2
Cone crusher (CC)	0.47	10000	0.95	0.60	10000	0.987
Roll crusher (RC)	0.79	2083	0.882	0.57	4000	0.924
Rotor beater mill (RBM)	0.34	3150	0.911	0.37	4000	0.887
Screen mill (SM)	0.44	2000	0.928	0.44	2291	0.961

Table 3: RR parameters for the two samples as comminuted by different devices

	L1			L2		
Device	*b*	*x'*	R^2	*b*	*x'*	R^2
Cone crusher (CC)	0.00	6000	0.755	1.55	3600	1.000
Roll crusher (RC)	3.80	896	0.973	2.90	996	1.000
Rotor beater mill (RBM)	0.95	552.30	1.000	1.30	527	1.000
Screen mill (SM)	1.73	596.24	0.999	1.60	520	1.000

In terms of the spread of size distribution as indicated by RR model parameters (Table 3), RC products were more uniformly distributed compared to products from other devices, for both samples (i.e. larger *b*). Also, the RBM products were more scattered than products from other devices (i.e. smaller *b*). The results indicate that the composition of individual ores affected the comminution products PSDs since different PSD model parameters were obtained for samples comminuted by same devices. This is in agreement with previous studies on chromite ores (Taşdemir and Taşdemir, 2009). The results are also in agreement with previous studies highlighting that GGS model is best at describing products from single-pass devices (low-energy events) such as cone and jaw crushers, where the effective breakage modes are cleavage and abrasion and that RR model is best at describing products from retention type devices (high-energy events) such as beater, hammer and ball mills where the main breakage mode is only shattering (Yue and Klein, 2005).

Liberation Characteristics

In this section, the mineral liberation characteristics of the two samples (L1 and L2) for the rotor beater mill products are presented. It has to be noted that all measurements for particle size and mineral grain size distributions are based on the Equivalent Circle Diameter (ECD). On the other hand, the liberation distribution is based on particle composition as mica is sorted by magnetic separation, which is sensitive to particle composition by volume (Leißner *et al*., 2016a, 2012).

Figure 3(a) presents the enrichment characteristics of Lithium containing Zinnwaldite phase with particle size. The results indicate that, for both samples, Zinnwaldite phase is more enriched in the fraction < 250 µm. Further, below 100 µm, Zinnwaldite is more enriched for L2 than L1. This implies that good recovery of Zinnwaldite mineral can be achieved if the ores are milled to less than 250 µm.

The mineral grain size distributions for L1 mineral phases are presented in Figure 3(b). The grain size distributions of Zinnwaldite from the two samples are also included for comparison. It is revealed that the grain size distribution of Zinnwaldite in sample L2 is finer than that in sample L1. This implies that more milling is required for better liberation of Zinnwaldite from L2 ore sample (i.e. small liberation size) than that for L1. Further, the the mineral grain size distribution of quartz closely follows size distribution of the host particles. Therefore, this main gangue shows a good liberation from the others (i.e. Most of the energy is lost in milling of the gangue material).

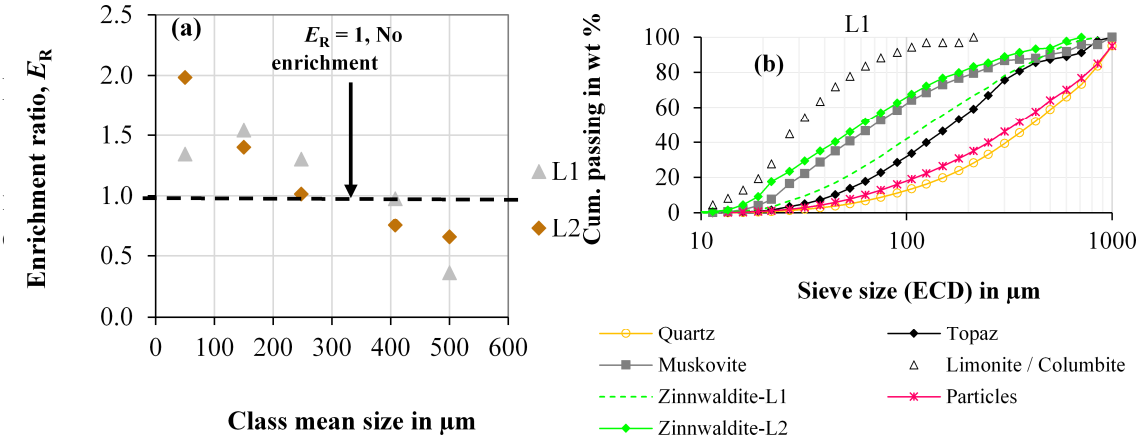

Figure 3: (a) Zinnwaldite enrichment with particle size. (b) Mineral grain size distributions (MGSD) for L1 mineral phases (i.e. also with Zinnwaldite MGSD from both samples).

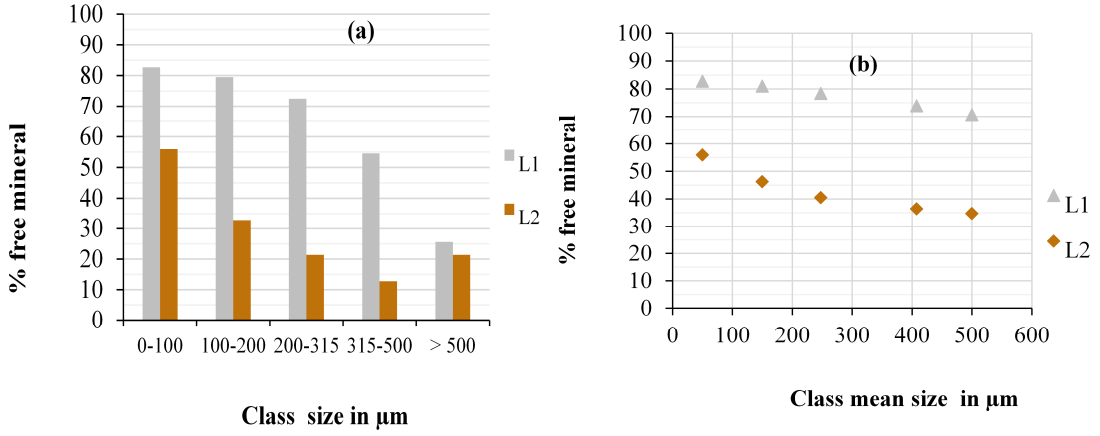

Figure 4: (a) Zinnwaldite fractional liberation. (b) Zinnwaldite cumulative liberation based. Both are based on 95-100 % liberation class.

Figure 4(a) and (b) show the fractional and cumulative liberation, respectively, for the valuable Zinnwaldite phase. In overall, better liberation of Zinnwaldite is observed for L1 compared to L2. For example, for the fractional liberation, approx. > 70 % free Zinnwaldite could be achieved in the fraction -315 + 200 µm for L1 compared to only 20 % that could be achieved for L2 for the same fraction. At first this might be linked to differences in Zinnwaldite mineral grain size in the two samples (i.e. in Figure 3(b), differences in mineralogical composition (Table 1) as well as the nature of spread of the size distribution (see RR parameters in Table 3).

Further, the ratios between geometric mean sizes of the feed to the rotor beater mill to that of the sieved fractions (i.e. reduction ratio) was calculated for the two samples and related with the cumulative Zinnwaldite liberation as shown in Figure 5. The result indicates that L1 had higher reduction ratio than L2 implying that L1 sieved fractions were finer than L2 fractions.

The proportion into which the valuable mineral, Zinnwaldite, is locked to other minerals in the ores is presented in Figure 6. For both samples, Zinnwaldite is mainly locked to Quartz and Muscovite. The locking trend shows that for both samples,

Zinnwaldite locking with Quartz increases with particle size, while locking to Muscovite decreases with increase in particle size. This is due to the mineralization of the deposit where Zinnwaldite was overgrown and replaced by Muscovite in a younger greisenization state (Sandmann and Gutzmer, 2013). Therefore, the fracture of Zinnwaldite-Muscovite is less favorable than associations to other minerals. Also a notable difference in Zinnwaldite locking can be observed for the mineral phase Topaz, where for sample L1 locking increases with particle size, while for L2 is the opposite. No significant differences between the two samples for the locking of Zinnwaldite into mineral phases Limmonite/Columbite and the minor phase ``other``. Hence the variation in locking characteristics of the valuable phase displayed from the two samples might also be the cause for differences in Zinnwaldite liberation indicated in Figure 4.

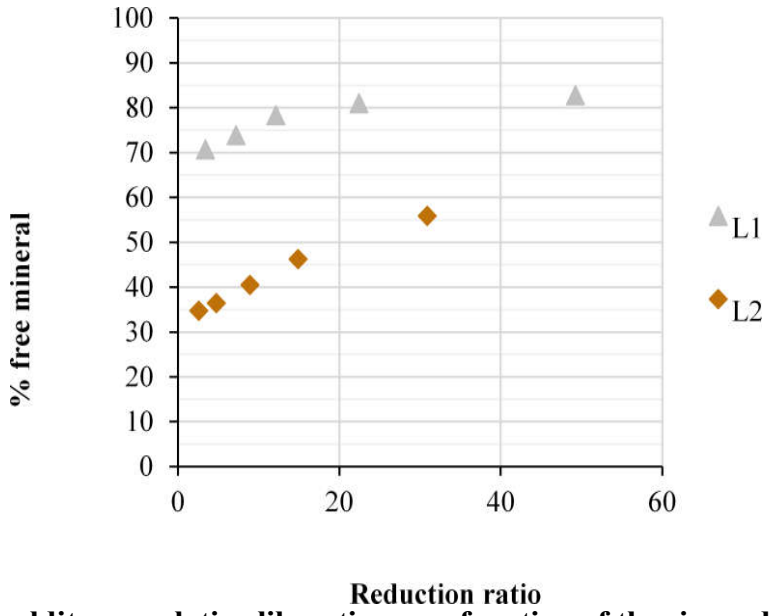

Figure 5: Zinnwaldite cumulative liberation as a function of the size reduction ratio for the two samples.

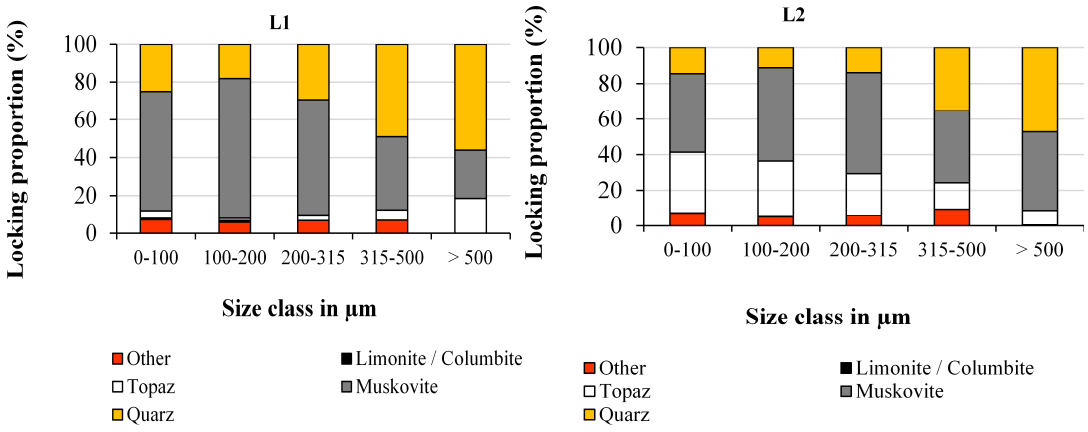

Figure 6: Locking of Zinnwaldite into other minerals for L1 and L2 ore samples.

CONCLUSIONS

Two lithium bearing-mica ore samples were comminuted by different devices and products size distributions evaluated by Gates-Gaudin-Schuhmann (GGS) and Rosin-Rammler (RR) models. The liberation characteristics were evaluated for products from one device; the rotor beater mill. The comminution results showed that the rotor beater mill, roller crusher and screen mill products were better described by RR model for both ores. Further, the cone crusher products for sample L1 were better described by GSS model, while that for L2 were better described by RR model. Different PSD model parameters were obtained for samples comminuted by same devices indicating that the composition of individual ore affected the comminution products. The observed differences in the Zinnwaldite liberation for the two samples could be linked to respective differences in the nature of mineral association, reduction ratio and the spread of the size distribution. These results mean that, depending on the dominant breakage mode, mineralogical characteristics, and feed size, different PDSs were obtained by different comminution devices for the investigated ores. Hence, GGS model was best at describing products from low-energy events (CC), whereas, RR model was best at describing products from high-energy events (RC, RBM, and SM). Also, the results imply that good recovery of Zinnwaldite mineral can be achieved if both ores are milled to less than 250 µm.

ACKNOWLEDGEMENTS

The authors gratefully acknowledge the Federal Ministry of Education and Research (BMBF) for the funding of the project "HybrideLithiumgewinnung" (03WKP18A). The authors would also like to thank the Department of Mineralogy, TU Bergakademie Freiberg for measurement of mineral liberation for the material. Furthermore, the Germany Academic Exchange Service (DAAD) is acknowledged for financing the first author for doctoral studies at TU Bergakademie Freiberg, Institute of Mechanical Process Engineering and Mineral Processing.

REFERENCES

Allen T. (2003). Powder Sampling and Particle Size Determination. 1st ed. eBook ISBN: 9780080539324. Elsevier, Amsterdam, The Netherlands.

Christelle V., Sandrine H., Marie-Noëlle P. and John D. (1997). Identification of the fragmentation mechanisms in wet-phase fine grinding in a stirred bead mill. Chem. Eng. Sci. 52: 3605–3612. https://doi.org/10.1016/S0009-2509(97)89693-5

Fandrich R., Gu Y., Burrows D. and Moeller K. (2007). Modern SEM-based mineral liberation analysis. Int. J. Miner. Process. 84: 310–320. https://doi.org/http://dx.doi.org/10.1016/j.minpro.2006.07.018

Gupta A. and Yan D.S. (2006). Introduction to Mineral Processing Design and Operation. Perth.

Katubilwa F.M. and Moys M.H. (2009). Effect of ball size distribution on milling rate. Miner. Eng. 22: 1283–1288. https://doi.org/http://dx.doi.org/10.1016/j.mineng.2009.07.008

Kaya E., Hogg R. and Kumar S. (2002). Particle Shape Modification in Comminution. KONA Powder Part. J. 20: 188–195. https://doi.org/10.14356/kona.2002021

King R.P. (2001). Modelling and Simulation of Mineral Processing Systems. 1st Edition, eBook ISBN**:** 9780080511849, Elsevier, Amsterdam, The Netherlands.

Kursun I. (2009). Particle Size and Shape Characteristics of Kemerburgaz Quartz Sands obtained by Sieving, Laser Diffraction, and Digital Image

Processing Methods. Miner. Process. Extr. Metall. Rev. 30: 346–360. https://doi.org/10.1080/08827500903149659

Leißner T., Bachmann K., Gutzmer J. and Peuker U.A. (2016a). MLA-based partition curves for magnetic separation. Minerals Engineering, 94: 94–103. https://doi.org/10.1016/j.mineng.2016.05.015

Leißner T., Hoang D.H., Rudolph M., Heinig T., Bachmann K., Gutzmer J., Schubert H. and Peuker U.A. (2016b). A mineral liberation study of grain boundary fracture based on measurements of the surface exposure after milling. Int. J. Miner. Process. 156: 3–13. https://doi.org/10.1016/j.minpro.2016.08.014

Leißner T., Rode S., Bachmann K., Gutzmer J. and Peuker U.A. (2012). Mineral processing of Lithium-bearing Mica. In 26th Int Min Proc Congress,. New Delhi, 2811–2820.

Lu P., Jefferson I.F., Rosenbaum M.S. and Smalley I.J. (2003). Fractal characteristics of loess formation: evidence from laboratory experiments. Eng. Geol., 69: 287–293. DOI: 10.1016/S0013-7952(02)00287-9

Macías-García A., Cuerda-Correa E.M. and Díaz-Díez M.A. (2004). Application of the Rosin–Rammler and Gates–Gaudin–Schuhmann models to the particle size distribution analysis of agglomerated cork. Mater. Charact. 52: 159–164. DOI: 10.1016/j.matchar.2004.04.007

Manohar B. and Sridhar B.S. (2001). Size and shape characterization of conventionally and cryogenically ground turmeric (Curcuma domestica) particles. Powder Technol. 120: 292–297. DOI: 10.1016/S0032-5910(01)00284-4

Napier-Munn T.J., Morrel S. and Kojovic T. (1996). Mineral Comminution Circuits: Their Operation and Optimisation, JKMRC Monograph Series in Mining and Mineral Processing 2. JKMRC, Queensland.

Narayanan S.S. and Whiten W.J. (1983). Breakage characteristics for ores for ball mill modelling,. Australas. Inst. Min. Metall. 31–39.

Rao D.V. (2011). Mineral Beneficiation: A Concise Basic Course. 1st Edition, Taylor and Francis, London. DOI: https://doi.org/10.1201/b11327

Sand G.W. and Subasinghe G.K.N. (2004). A novel approach to evaluating breakage parameters and modelling batch grinding. Miner. Eng. 17: 1111–1116. https://doi.org/http://dx.doi.org/10.1016/j.mineng.2004.06.019

Sandmann D. and Gutzmer J. (2013). Use of Mineral Liberation Analysis (MLA) in the Characterization of Lithium-Bearing Micas. Miner. Mater. Charact. Eng. 1: 285–292. https://doi.org/http://dx.doi.org/10.4236/jmmce.2013.16043

Taşdemir A. and Taşdemir T. (2009). A Comparative Study on PSD Models for Chromite Ores Comminuted by Different Devices. Part. Part. Syst. Charact. 26: 69–79. DOI: 10.1002/ppsc.200800035

Yue J. and Klein B. (2005). Particle breakage kinetics in horizontal stirred mills. Miner. Eng. 18: 325–331. https://doi.org/https://doi.org/10.1016/j.mineng.2004.06.009